

Synthesis, Characterization, and Novel Fluxional Mechanisms of Triosmium Clusters Containing the Highly Flexible Ligand $\text{Ph}_2\text{PC}_2\text{H}_4\text{SC}_2\text{H}_4\text{SC}_2\text{H}_4\text{PPh}_2$ (PSSP)

Roger Persson,[†] Marc J. Stchedroff,[†] Bettina Uebersezig,[†] Roberto Gobetto,[‡] Jonathan W. Steed,[§] Paul D. Prince,[§] Magda Monari,[⊥] and Ebbe Nordlander^{*,†}

[†]*Inorganic Chemistry Research Group, Chemical Physics, Center for Chemistry and Chemical Engineering, Lund University, Box 124, SE-221 Lund, Sweden,* [‡]*Dipartimento di Chimica Inorganica, Chimica Fisica e de Chimica dei Materiali, Università degli Studi di Torino, Via Pietro Giuria 7, 10125 Torino, Italy,* [§]*Department of Chemistry, University of Durham, U.K., and* [⊥]*Dipartimento di Chimica "G. Ciamician", Università degli Studi di Bologna, Via Selmi 2, I-40126 Bologna, Italy*

Received November 4, 2009

Treatment of $\text{Ph}_2\text{PC}_2\text{H}_4\text{SC}_2\text{H}_4\text{SC}_2\text{H}_4\text{PPh}_2$ (PSSP) with $[\text{Os}_3(\text{CO})_{11}(\text{NCMe})]$ under mild conditions yields $[\{\text{Os}_3(\text{CO})_{11}\}_2(\mu\text{-PSSP})]$, **1**, and $[\text{Os}_3(\text{CO})_{11}(\text{PSSP})]$, **2**. In cluster **1** the ligand links two trinuclear cluster subunits, coordinating via its phosphine moieties. In cluster **2**, the ligand is coordinated through one of the phosphine groups, while the remaining part of the PSSP ligand is oriented in a dangling mode. Treatment of $[\text{Os}_3(\text{CO})_{10}(\text{NCMe})_2]$ with PSSP yields $1,2\text{-}[\text{Os}_3(\text{CO})_{10}(\text{PSSP})]$, **3**. NMR data presented in this paper indicate that a concerted *cis/trans* isomerism with respect to the phosphines operates in the cluster. This type of process has not been observed previously for a bridging ligand, but has been detected in the case of corresponding triosmium clusters with bis-monodentate phosphine ligands. Oxidative decarbonylation of $[\{\text{Os}_3(\text{CO})_{11}\}_2(\mu\text{-PSSP})]$, **1**, with Me_3NO yields cluster $[\{\text{Os}_3(\text{CO})_{10}\}_2(\mu\text{-PSSP})]$, **4**. This cluster consists of two P,S-bridged cluster units. In solution at room temperature, **4** undergoes a slow rearrangement from a 1,2-bridging to a 1,1-chelating coordination mode. The crystal structures of clusters **1**, **3**, and **4** are reported.

Introduction

Multidentate phosphine-thiol or phosphine-thioether (P,S) ligands are of considerable interest since they are intrinsically asymmetric and potentially hemilabile.^{1–4} Such ligands have been shown to be potentially useful in catalytic alkylation, carbonylation, and coupling reactions.^{5,6} We are currently investigating the reactivity of phosphine-thioether ligands with polynuclear transition metal complexes. In particular, we want to determine to what extent the thioether moiety may compete with the phosphines as a ligand to one or several transition metal(s) in a low oxidation state. More-

over, the correlation of coordination modes of such ligands with the reactivity of the specific clusters is of general interest and is also central to different applications, e.g. development of new catalysts and potentially useful synthons in preparative chemistry.⁷ In recent studies on the coordination properties of the PS [$\text{PPh}_2(\text{CH}_2)_2\text{SMe}$]⁸ and PSP [$\text{PPh}_2(\text{CH}_2)_2\text{S}(\text{CH}_2)_2\text{PPh}_2$] ligands,⁹ we have found that the thioether moiety of the phosphine-thioether ligands can coordinate to a metal center only when the phosphine is already coordinated. On the other hand, prior coordination of the phosphine moiety (moieties) of these ligands may favor thioether coordination via the chelate effect. This is a useful way to coordinate inactive sulfur (or other donor atoms) to metal centers under mild conditions. For example, thienylphosphines may be used as “Trojan horses” to introduce

*Corresponding author. E-mail: Ebbe.Nordlander@chemphys.lu.se
Fax: +46 46 222 4439.

(1) (a) Brown, M. P.; Bolby, P. A.; Harding, M. M.; Mathews, A. J.; Smith, A. K. *J. Chem. Soc., Dalton Trans.* **1993**, 1671. (b) Coleman, A. W.; Jones, A. W.; Dixneuf, P. H.; Brisson, C.; Bonnet, J. J.; Lavigne, G. *Inorg. Chem.* **1984**, *23*, 952.

(2) Johnson, B. F. G.; Lewis, J.; Monari, M.; Braga, D.; Grepioni, F.; Gradella, C. *J. Chem. Soc., Dalton Trans.* **1990**, 2863.

(3) (a) Cartwright, S.; Lucas, J. A.; Dawson, R. H.; Foster, D. F.; Harding, M. M.; Smith, A. K. *J. Organomet. Chem.* **1986**, *302*, 403. (b) Corey, E. R.; Dahl, L. F. *Inorg. Chem.* **1962**, *1*, 521. (c) Lucas, J. A.; Foster, D. F.; Harding, M. M.; Smith, A. K. *J. Chem. Soc., Chem. Commun.* **1984**, 949.

(4) Johnson, B. F. G. *J. Chem. Soc., Chem. Commun.* **1976**, 211.

(5) Hauptman, E.; Fagan, P. J.; Marshall, W. *Organometallics* **1999**, *18*, 2061–2073, and references therein.

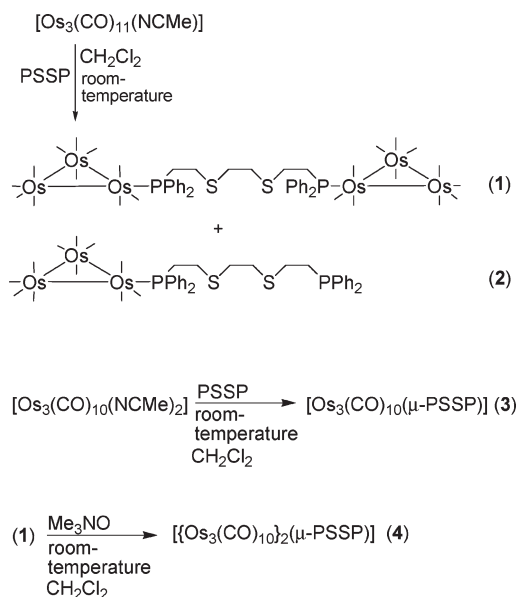
(6) Dilworth, J. R.; Wheatley, N. *Coord. Chem. Rev.* **2000**, *199*, 89.

(7) (a) Moreno, M. A.; Haukka, M.; Jaaeskelainen, S.; Vuoti, S.; Pursiainen, J.; Pakkanen, T. A. *J. Organomet. Chem.* **2005**, *690* (16), 3803–3814. (b) Sola, J.; Reves, M.; Riera, A.; Verdagner, X. *Angew. Chem., Int. Ed.* **2007**, *46* (26), 5020–5023, and references therein. (c) Lam, F. L.; Au-Yeung, T. T.-L.; Kwong, F. Y.; Zhongyuan, Z.; Wong, K. Y.; Chan, A. S. C. *Angew. Chem., Int. Ed.* **2008**, *47* (7), 1280–1283. (d) Cheung, H. Y.; Yu, W.-Y.; Lam, F. L.; Au-Yeung, T. T.-L.; Zhongyuan, Z.; Chan, T. H.; Chan, A. S. C. *Org. Lett.* **2007**, *9* (21), 4295–4298. (e) Nakamura, S.; Fukuzumi, T.; Toru, T. *Chirality* **2003**, *16* (1), 10–12. (f) Zeng, W.; Zhou, Y.-G. *Tetrahedron Lett.* **2007**, *48* (26), 4619–4622.

(8) Persson, R.; Monari, M.; Gobetto, R.; Russo, A.; Aime, S.; Calhorda, M. J.; Nordlander, E. *Organometallics* **2001**, *20*, 4150.

(9) Persson, R. Ph.D. Thesis, Lund University, **2009**.

Scheme 1. Preparation of Compounds 1–4



thienyl moieties in low-valent metal complexes;^{10,11} initial coordination by the phosphine moiety of a thienylphosphine permits, in some cases, subsequent coordination via the thienyl sulfur.¹¹

The ligand bis(diphenylphosphinodiethylene)ethylenedisulfide (PSSP) is closely related to the above-mentioned P, S-donor ligands. It has considerable flexibility, an unusual chain length, and four potential donor atoms. We were interested in investigating whether PSSP exhibits coordinative behavior similar to that of PS and PSP. Here, we report the results of the reaction of PSSP with the mono- and bis-acetonitrile derivatives of $[\text{Os}_3(\text{CO})_{12}]$ ¹² as well as some further reactions of the resultant products.

Results and Discussion

Synthesis of $[\{\text{Os}_3(\text{CO})_{11}\}_2(\mu\text{-PSSP})]$ (1), $[\text{Os}_3(\text{CO})_{11}(\text{PSSP})]$ (2), $[\text{Os}_3(\text{CO})_{10}(\mu\text{-PSSP})]$ (3), and $[\{\text{Os}_3(\text{CO})_{10}\}_2(\mu\text{-PSSP})]$ (4). Treatment of $[\text{Os}_3(\text{CO})_{11}(\text{NCMe})]$ with PSSP at room temperature in dichloromethane gave $[\{\text{Os}_3(\text{CO})_{11}\}_2(\mu\text{-PSSP})]$, **1**, and $[\text{Os}_3(\text{CO})_{11}(\text{PSSP})]$, **2** (Scheme 1). The predominant species was dependent on the stoichiometric ratios of the reactants. Thus, cluster **1** is obtained in high yield as a yellow crystalline compound by reacting PSSP with two equivalents of $[\text{Os}_3(\text{CO})_{11}(\text{NCMe})]$. On the other hand, the room-temperature reaction of $[\text{Os}_3(\text{CO})_{11}(\text{NCMe})]$ with one equivalent of PSSP gave a relatively low yield (9%, after separation) of **2** as an orange oil. Treatment of $[\text{Os}_3(\text{CO})_{10}(\text{NCMe})_2]$ with PSSP at room temperature in dichloromethane

yielded $[\text{Os}_3(\text{CO})_{10}(\mu\text{-PSSP})]$ (**3**) (Scheme 1). On treatment of **1** with two equivalents of the oxo-transfer reagent trimethylamine *N*-oxide, $[\{\text{Os}_3(\text{CO})_{10}\}_2(\mu\text{-PSSP})]$ (**4**) is obtained as an orange solid in ca. 60% yield (Scheme 1). All the products are air and thermally stable and can be separated on silica.

Characterization of $[\{\text{Os}_3(\text{CO})_{11}\}_2(\mu\text{-PSSP})]$ (1). The ¹H NMR spectrum of compound **1** showed the methylene signals as three complex multiplets at δ 2.27, 2.49, and 2.82. The ³¹P{¹H} NMR spectrum exhibits a singlet at δ -10.9, indicating that the phosphorus atoms are equivalent and that the solution structure of the cluster is symmetric. This is consistent with two cluster subunits linked by a bridging ligand. The mass spectrum shows an isotopic envelope at 2276 amu, in agreement with the values obtained in the simulated spectrum, and the IR spectrum is similar to that previously observed for $[\{\text{Os}_3(\text{CO})_{11}\}_2(\text{L})]$ (where L is a bidentate phosphine ligand).¹³ We have been unable to freeze out any conformers (173 K, 500 MHz) of **1**; it is possible that the interactions between phenyl moieties of the ligand (*vide infra*) are responsible for this. Another possibility that cannot be ruled out with such a flexible ligand is that the ligand chain is highly mobile even at very low temperatures, thus averaging any potential conformers on the NMR time scale.

Crystal and Molecular Structure of $[\{\text{Os}_3(\text{CO})_{11}\}_2(\mu\text{-PSSP})]$ (1). A single-crystal X-ray study was carried out on **1** in order to confirm the proposed structure for the cluster. The molecular structure of **1** (Figure 1, relevant bond lengths and angles in Table 1) confirms that the diphosphine ligand is bridging two triosmium subunits, being coordinated in a $\kappa^1(\text{P})$ -mode. Similar diphosphine-bridged dimers have been prepared by us⁹ and by other groups.^{14–18,25–27} The phosphine moieties coordinate to equatorial sites on each triosmium unit, as has been previously found in related $[\text{Os}_3(\text{CO})_{11}(\text{PR}_3)]$ species.^{17–19,21–24} The two triosmium triangles are oriented approximately at 90° to each other. The

(13) Kabir, S. E. Ph.D. Thesis, University of London, 1986.

(14) Bruce, M. I.; Hambley, T. W.; Nicholson, B. K.; Snow, M. R. *J. Organomet. Chem.* **1982**, 235, 83.

(15) Ang, S. G.; Zhong, X.; Ang, H. G. *J. Chem. Soc., Dalton Trans.* **2001**, 1151.

(16) Ang, S. G.; Zhong, X.; Ang, H. G. *Inorg. Chem.*, **2002**, 41 (14).

(17) Deeming, A. J.; Donovan-Mtunzi, S.; Kabir, S. E. *J. Organomet. Chem.* **1987**, 333, 253.

(18) Kabir, S. E.; Miah, A.; Nesa, L.; Uddin, K.; Hardcastle, K. I.; Rosenberg, E.; Deeming, A. J. *J. Organomet. Chem.* **1995**, 492, 41–51.

(19) Deeming, A. J.; Hardcastle, K. I.; Kabir, S. E. *J. Chem. Soc., Dalton Trans.* **1988**, 827.

(20) (a) Bruce, M. I.; Liddell, M. J.; Hughes, C. A.; Skelton, B. W.; A. H. White, A. H. *J. Organomet. Chem.* **1988**, 347, 157. (b) Bruce, M. I.; Addick, J. M.; Hughes, C. A.; Patrick, J. A.; Skelton, B. W.; White, A. H. *J. Organomet. Chem.* **1988**, 347, 181. (c) Bruce, M. I.; Lidell, M. J.; Shawkataly, O.; Hughes, C. A.; Skelton, B. W.; White, A. H. *J. Organomet. Chem.* **1988**, 347, 207.

(21) (a) Alex, R. F.; Pomeroy, R. K. *Organometallics* **1987**, 6, 2437. (b) Alex, R. F.; Einstein, F. W. B.; Jones, R. H.; Pomeroy, R. K. *Inorg. Chem.* **1987**, 19, 3175. (c) Alex, R. F.; Pomeroy, R. K. *J. Organomet. Chem.* **1985**, 284, 379. (d) Alex, R. F.; Pomeroy, R. K. *Organometallics* **1982**, 3, 453.

(22) Deeming, A. J. In *Comprehensive Organometallic Chemistry II*; Abel, E. W.; Stone, F. G. A.; Wilkinson, G., Eds.; Elsevier: Oxford, 1995; Vol. 7, Chapter 12.

(23) (a) Deeming, A. J.; Donovan-Mtunzi, S.; Kabir, S. E.; Manning, P. J. *J. Chem. Soc., Dalton Trans.* **1996**, 1037. (b) Deeming, A. J.; Donovan-Mtunzi, S.; Kabir, S. E. *J. Organomet. Chem.* **1985**, C43, 281.

(24) Leong, W. K.; Liu, Y. *J. Organomet. Chem.* **1999**, 584, 174.

(25) (a) Deeming, A. J.; Donovan-Mtunzi, S.; Kabir, S. E. *J. Organomet. Chem.* **1984**, 276, C65. (b) Deeming, A. J.; Kabir, S. E. *J. Organomet. Chem.* **1988**, 340, 359.

(26) Johnson, B. F. G.; Lewis, J.; Reichert, B. E.; Schorpp, K. T. *J. Chem. Soc., Dalton Trans.* **1976**, 1403.

(10) (a) Arce, A. J.; Deeming, A. J.; DeSanctis, Y.; Speel, D. M.; DiTrapani, A. *J. Organomet. Chem.* **1999**, 2, 370. (b) Arce, A. J.; Karam, A.; DeSanctis, Y.; Capparelli, M. V.; Deeming, A. J. *Inorg. Chim. Acta* **1999**, 2, 277. (c) Arce, A. J.; Arrojo, P.; DeSanctis, Y.; Marquez, M.; Deeming, A. J. *J. Organomet. Chem.* **1994**, 1, 159. (d) Deeming, A. J.; Nuel, D.; Powell, N. I.; Whittaker, C. *J. Chem. Soc., Dalton Trans.* **1992**, 5, 757. (e) Deeming, A. J.; Powell, N. I.; Arce, A. J.; DeSanctis, Y.; Manzur, J. *J. Chem. Soc., Dalton Trans.* **1991**, 12, 3381.

(11) (a) King, J. D.; Monari, M.; Nordlander, E. *J. Organomet. Chem.* **1999**, 57, 272. (b) Kiriakidou, K.; Plutino, M. R.; Prestopino, F.; Monari, M.; Johansson, M.; Elding, L. I.; Valls, E.; Gobetto, R.; Aime, S.; Nordlander, E. *Chem. Commun.* **1998**, 2721.

(12) Dawson, P. A.; Johnson, B. F. G.; Lewis, J.; Puga, J.; Raithby, P. R.; Rosales, M. J. *J. Chem. Soc., Dalton Trans.* **1982**, 233.

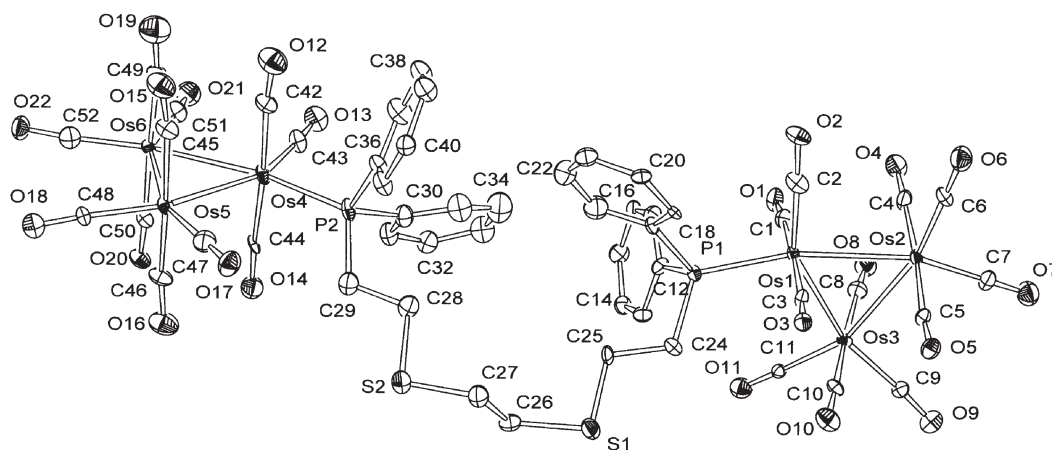


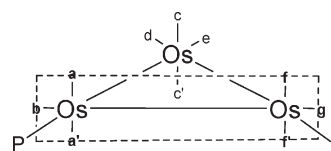
Figure 1. ORTEP drawing of the molecular structure of $[\{\text{Os}_3(\text{CO})_{11}\}_2(\mu\text{-PSSP})]$, **1**. Hydrogen atoms have been omitted for clarity.

Table 1. Selected Bond Lengths (Å) and Angles (deg) for $[\{\text{Os}_3(\text{CO})_{11}\}_2(\mu\text{-PSSP})]$, **1**

Os(1)–Os(2)	2.8752(9)	Os(4)–C(44)	1.91(2)
Os(1)–Os(3)	2.8982(9)	Os(4)–C(42)	1.94(2)
Os(2)–Os(3)	2.889(1)	Os(5)–C(48)	1.92(2)
Os(4)–Os(6)	2.883(1)	Os(5)–C(47)	1.92(2)
Os(4)–Os(5)	2.908(1)	Os(5)–C(46)	1.92(2)
Os(5)–Os(6)	2.890(1)	Os(5)–C(45)	1.96(2)
Os(1)–P(1)	2.351(4)	Os(6)–C(50)	1.96(2)
P(2)–Os(4)	2.355(5)	Os(6)–C(52)	1.90(2)
Os(1)–C(2)	1.85(2)	Os(6)–C(51)	1.95(2)
Os(1)–C(1)	1.96(2)	Os(6)–C(49)	1.95(2)
Os(1)–C(3)	1.970(19)	S(1)–C(25)	1.77(2)
Os(2)–C(6)	1.896(19)	S(1)–C(26)	1.88(2)
Os(2)–C(7)	1.926(19)	P(1)–C(18)	1.83(2)
Os(2)–C(4)	1.98(2)	P(1)–C(12)	1.84(2)
Os(2)–C(5)	1.986(19)	P(1)–C(24)	1.86(2)
Os(3)–C(9)	1.890(17)	S(2)–C(27)	1.83(2)
Os(3)–C(11)	1.922(17)	S(2)–C(28)	1.92(2)
Os(3)–C(8)	1.94(2)	P(2)–C(36)	1.82(2)
Os(3)–C(10)	1.95(2)	P(2)–C(29)	1.83(2)
Os(4)–C(43)	1.86(2)	P(2)–C(30)	1.87(2)
C(18)–P(1)–C(12)	104.5(8)	C(29)–P(2)–Os(4)	117.7(7)
C(18)–P(1)–C(24)	102.7(9)	C(3)0–P(2)–Os(4)	112.7(7)
C(12)–P(1)–C(24)	104.1(9)	C(25)–S(1)–C(26)	97.3(9)
C(18)–P(1)–Os(1)	113.8(6)	C(27)–S(2)–C(28)	100(1)
C(12)–P(1)–Os(1)	114.9(7)	C(8)–Os(3)–C(10)	174.9(8)
C(24)–P(1)–Os(1)	115.5(6)	C(44)–Os(4)–C(42)	174.0(9)
C(36)–P(2)–C(29)	105.3(10)	C(46)–Os(5)–C(45)	177.4(9)
C(36)–P(2)–C(30)	106.9(10)	C(49)–Os(6)–C(50)	178.2(8)
C(29)–P(2)–C(30)	99.7(11)	C(52)–Os(6)–Os(4)	162.9(7)
C(36)–P(2)–Os(4)	113.1(7)	C(4)–Os(2)–C(5)	175.7(7)

arrangement of the phenyl groups appears to stabilize the structure and lock it into the conformation detected in the crystal structure. The two pairs of phenyl groups are oriented roughly edge-to-face to each other. The aliphatic part of the ligand is oriented in a symmetric way. The sulfur atoms are not within bonding distance to any osmium atom. As is frequently observed in $[\text{Os}_3(\text{CO})_{11}(\text{PR}_3)]$ clusters,^{20,22} the *cis* bonds relative to the phosphorus-donor ligands are longer than remaining metal–metal bonds due to the steric bulk of the phosphine ligands, i.e. Os(1)–Os(3) 2.8982(9) Å, Os(4)–

Scheme 2. Proposed Classical Merry-go-Round Fluxional Process for $[\text{Os}_3(\text{CO})_{11}(\text{PSSP})]$ Involving Sites *a*, *f*, *b*, and *g*^a



^aSignals with shifts 193.1, 185.4, 176.3, and 170.2; see Figure 2.

Os(5) 2.9077(11) Å. The Os(1)–Os(3) and Os(4)–Os(5) separations are also longer than the Os–Os separations in the parent cluster $[\text{Os}_3(\text{CO})_{12}]$ [2.877(3) Å].²⁸ The Os–P distances [Os(1)–P(1) 2.351(4) Å and Os(4)–P(2) 2.355(5) Å] fall in the range 2.285–2.399 Å, which is typical for these bonds.

Characterization of $[\text{Os}_3(\text{CO})_{11}(\text{PSSP})]$ (2**).** The mass spectrum of cluster **2** shows an isotopic envelope at 1426 amu, consistent with the simulated spectrum. The IR spectrum of **2** is similar to that previously observed for **1** and $[\text{Os}_3(\text{CO})_{11}(\text{L})]$ (P = PPh₃, P(OMe)₃) clusters.²¹ The ³¹P{¹H} NMR shows two singlets at δ –17.3 and –10.2 attributable to free and coordinated phosphine moieties, respectively. The ¹³CO{¹H} variable-temperature spectra show the expected fluxional behavior and confirm a simple κ¹(P) coordination mode. The low-temperature limiting spectrum (500 MHz, 213 K, CDCl₃) shows eight carbonyl signals representing 11 carbonyls in a 2:2:2:1:1:1:1:1 pattern at δ 193.1 (²J_{P–C} ≈ 8 Hz) *a*, 185.4 *f*, 183.9 *c*, 176.8 *b*, 176.7 *d*, 172.8 *h*, 172.4 *e*, and 170.2 *g* (the letters refer to assignments according to Scheme 2); see Figure 2.²¹ The three high-frequency signals are assigned to the axial carbonyls on the basis of chemical shifts and integral values (2H). The CO signal at highest frequency (δ 193.1) shows phosphorus coupling (²J_{C–P} 7.9 Hz), whereas the five singlets (integral 1) are assigned to equatorial carbonyl ligands. On raising the temperature to 273 K, the signals originating from the six carbonyls along one edge of the cluster coalesce in a classical merry-go-round process, involving sites *a*, *f*, *b*, and *g* (see Scheme 2). The remaining carbonyl signals are assigned in accordance with assignments of similar $[\text{Os}_3(\text{CO})_{11}(\text{L})]$ (L = phosphine or phosphite) compounds;^{21a} see Scheme 2. Line-shape analysis confirms the presence of the merry-go-round process involving carbonyls *a*, *f*, *b*, and *g* and affords a value for the carbonyl exchange activation energy of 49.3 ± 2.0 kJ/mol.

(27) (a) Watson, W. H.; Wu, G.; Richmond, M. G. *Organometallics* **2006**, *25*, 930–945. (b) Watson, W. H.; Wu, G.; Richmond, M. G. *Organometallics* **2005**, *24*, 5431–5439. (c) Watson, W. H.; Poola, B.; Richmond, M. G. *J. Organomet. Chem.* **2006**, *691*, 4676–4685.

(28) (a) Churchill, M. R.; Lashewycz, R. A.; Richter, S. I.; Shapley, J. R. *Inorg. Chem.* **1980**, *19*, 1277. (b) Puga, J.; Arce, A. J.; Braga, D.; Centritto, N.; Grepioni, F.; Castillo, R.; Ascanio, J. *Inorg. Chem.* **1987**, *26*, 867. (c) Homanen, P.; Persson, R.; Haukka, M.; Pakkanen, T. A.; Nordlander, E. *Organometallics* **2000**, *19*, 5568–5574.

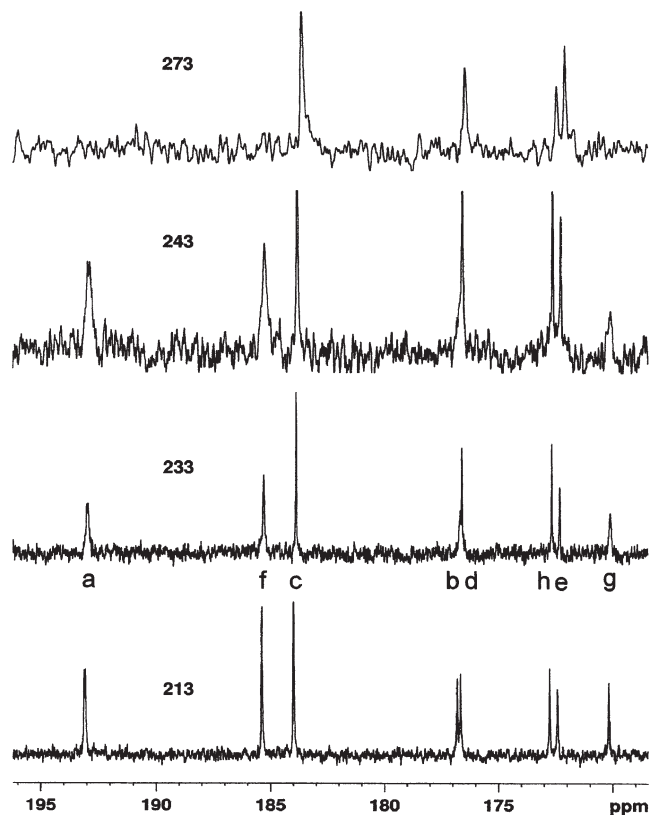


Figure 2. Low-temperature-limiting ^{13}C NMR spectrum (125 MHz, 213 K, CDCl_3) for $[\text{Os}_3(\text{CO})_{11}(\text{PSSP})]$, **2**, shows eight signals representing 11 carbonyl ligands in a 2:2:2:1:1:1:1:1 pattern: δ 193.1(2), 185.4(2), 183.9(2), 176.8(1), 176.7(1), 172.8(1), 172.4(1), 170.2(1) (figures in parentheses refer to the relative intensities).

Characterization of $[\text{Os}_3(\text{CO})_{10}(\mu\text{-PSSP})]$ (3**).** The mass spectrum of **3** shows an isotopic envelope at 1369 amu consistent with the value of 1370 amu for a cluster of principal formula $[\text{Os}_3(\text{CO})_{10}(\mu\text{-PSSP})]$. The IR spectrum of **3** in CH_2Cl_2 is slightly different from those of $[\text{Os}_3(\text{CO})_{10}(\mu\text{-PSP})]^9$ and $[\text{Os}_3(\text{CO})_{10}(\mu\text{-P-P})]$ ($\text{P-P} = \text{dpppe}$ or dppp),¹³ suggesting that the solution structure of **3** differs from those of the above-mentioned clusters, where the two phosphine moieties are coordinated in equatorial *cis* positions (1,2-*cis*, *cis*) relative to each other.

The $^{31}\text{P}\{^1\text{H}\}$ NMR spectrum of **3** recorded at room temperature shows a broad resonance at $\delta -8$ (and a minor resonance at $\delta -10$) indicating ligand fluxionality on the NMR time scale (Figure 3). This fluxional process can be frozen out at low temperature (213 K), and the static spectrum shows three resonances at $\delta -5.5$, -9.4 , and -10.1 . The three ^{31}P chemical shifts demonstrate that the two phosphorus atoms are nonequivalent (*vide infra*). It is reasonable to assume that both coordinate to the osmium triangle²² in equatorial positions. There are then four possible isomers that may, in principle, be observed for an $[\text{Os}_3(\text{CO})_{10}(\text{L})_2]$ system (see Figure 4). Disubstituted clusters of formula $[\text{Os}_3(\text{CO})_{10}(\text{PR}_3)_2]$ ($\text{PR}_3 = \text{phosphine}$ or phosphite) are known to exist as interconverting *trans,trans* and *cis,trans* isomers, but for bidentate phosphines, only the bridged *cis,cis* and chelating *cis,cis* coordination modes have been observed.^{13,17–19,23} Recently, the crystal structure of *cis,trans* $[\text{Os}_3(\text{CO})_{10}(\text{PPh}_3)_2]$, known for some time from NMR data, was published.²⁴ In $[\text{Os}_3(\text{CO})_{10}(\text{PSSP})]$ the

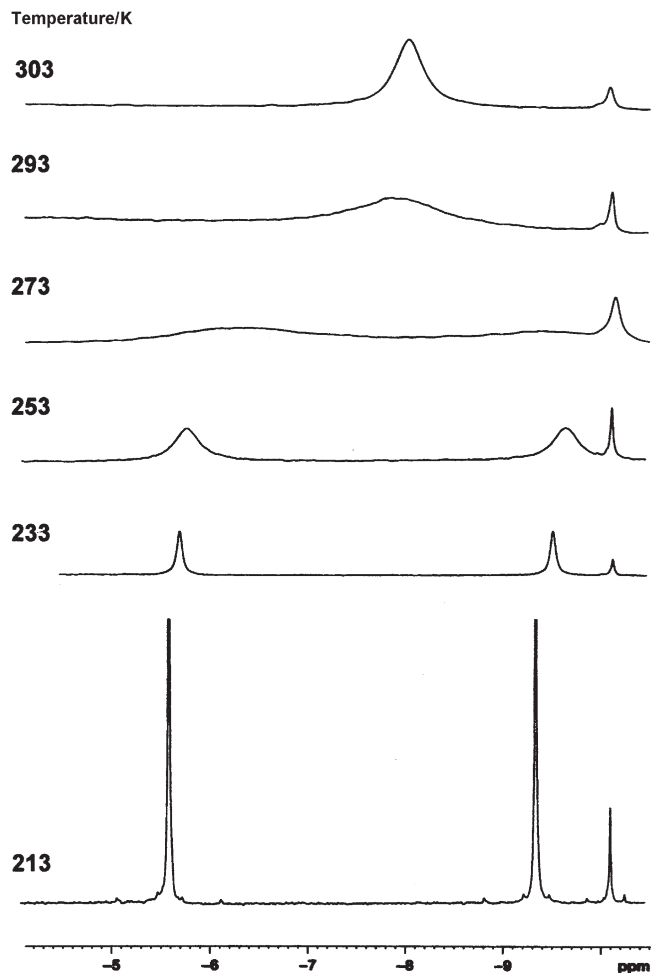


Figure 3. Variable-temperature $^{31}\text{P}\{^1\text{H}\}$ NMR of 1,2- $[\text{Os}_3(\text{CO})_{10}(\text{PSSP})]$, **3**.

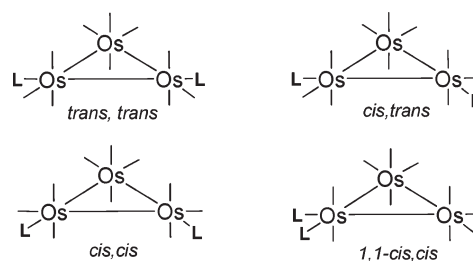


Figure 4. Four possible isomers that may, in principle, be observed for an $[\text{Os}_3(\text{CO})_{10}(\text{L})_2]$ system.

bridging PSSP ligand forms an unusual 12-membered ring incorporating also the two phosphorus-coordinated osmium atoms. Such a large ring may in principle permit the ligand to coordinate in the 1,2-*cis,trans* mode and/or even in the 1,2-*trans,trans* mode. In order to identify the coordination mode of the PSSP ligand in **3** in the solid state, a single-crystal X-ray study was undertaken.

Crystal and Molecular Structure of $[\text{Os}_3(\text{CO})_{10}(\mu\text{-PSSP})]$ (3**).** The molecular structure of **3** is shown in Figure 5, and selected bond lengths and angles are listed in Table 2. Two independent chiral molecules are present in the asymmetric unit. They are related by quasi-reflection through a plane orthogonal to the Os_3P_2 plane and therefore can be a pair of enantiomers. The chirality originates from the tilting in

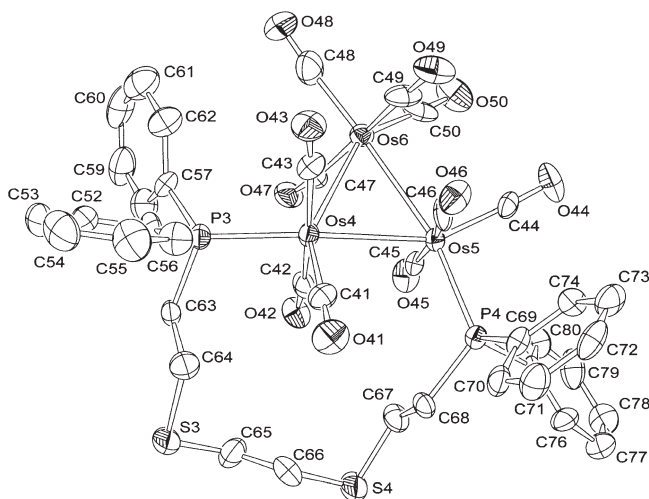


Figure 5. ORTEP drawing of one of the two conformers of 1,2- $[\text{Os}_3(\text{CO})_{10}(\text{PSSP})]$, **3**. Hydrogen atoms have been omitted for clarity.

Table 2. Selected Bond Lengths (Å) and Angles (deg) for $[\text{Os}_3(\text{CO})_{10}(\mu\text{-PSSP})]$, **3**

molecule 1		molecule 2	
Os(1)–Os(2)	2.9046(6)	Os(4)–Os(5)	2.9051(6)
Os(1)–Os(3)	2.8770(6)	Os(4)–Os(6)	2.9087(6)
Os(2)–Os(3)	2.9019(6)	Os(5)–Os(6)	2.8889(6)
Os(1)–C(1)	1.864(12)	Os(4)–C(41)	1.87(1)
Os(1)–C(2)	1.886(14)	Os(4)–C(42)	1.95(1)
Os(1)–C(3)	1.947(13)	Os(4)–C(43)	1.92(1)
Os(1)–P(1)	2.358(3)	Os(4)–P(3)	2.336(3)
Os(2)–C(4)	1.89(1)	Os(5)–C(44)	1.87(1)
Os(2)–C(5)	1.91(1)	Os(5)–C(45)	1.99(1)
Os(2)–C(6)	1.86(1)	Os(5)–C(46)	1.91(1)
Os(2)–P(2)	2.338(3)	Os(5)–P(4)	2.361(3)
Os(3)–C(7)	1.88(1)	Os(6)–C(47)	1.96(1)
Os(3)–C(8)	1.88(1)	Os(6)–C(48)	1.90(2)
Os(3)–C(9)	1.91(1)	Os(6)–C(49)	1.93(2)
Os(3)–C(10)	1.87(1)	Os(6)–C(50)	1.92(2)
P(1)–C(11)	1.821(6)	P(4)–C(69)	1.830(6)
P(1)–C(17)	1.841(6)	P(4)–C(75)	1.834(6)
P(1)–C(23)	1.83(1)	P(4)–C(68)	1.86(1)
P(2)–C(28)	1.81(1)	P(3)–C(57)	1.788(6)
P(2)–C(35)	1.814(6)	P(3)–C(51)	1.839(6)
P(2)–C(29)	1.831(6)	P(3)–C(63)	1.88(1)
S(1)–C(24)	1.78(1)	S(4)–C(66)	1.81(1)
S(1)–C(25)	1.80(1)	S(4)–C(67)	1.80(1)
S(2)–C(26)	1.80(1)	S(3)–C(65)	1.75(1)
S(2)–C(27)	1.81(1)	S(3)–C(64)	1.82(1)
S(1)···S(2)	4.433(5)	S(3)···S(4)	4.417(5)
C(11)–P(1)–Os(1)	117.7(3)	C(69)–P(4)–Os(5)	112.4(3)
C(23)–P(1)–Os(1)	119.8(4)	C(75)–P(4)–Os(5)	118.1(3)
C(17)–P(1)–Os(1)	113.2(3)	C(68)–P(4)–Os(5)	119.8(4)
C(24)–S(1)–C(25)	104.6(6)	C(67)–S(4)–C(66)	102.4(6)
C(1)–Os(1)–Os(3)	94.4(3)	C(44)–Os(5)–Os(6)	96.4(3)
C(1)–Os(1)–P(1)	98.7(3)	C(44)–Os(5)–P(4)	95.8(3)
P(1)–Os(1)–Os(2)	107.85(7)	P(4)–Os(5)–Os(6)	107.95(7)
C(9)–Os(3)–Os(1)	97.9(3)	C(50)–Os(6)–Os(5)	90.0(4)
C(26)–S(2)–C(27)	101.5(5)	C(65)–S(3)–C(64)	100.7(6)
C(6)–Os(2)–P(2)	97.6(3)	C(41)–Os(4)–P(3)	98.7(4)
P(2)–Os(2)–Os(3)	112.93(7)	P(3)–Os(4)–Os(6)	114.57(7)
C(7)–Os(3)–Os(2)	102.7(3)	C(48)–Os(6)–Os(4)	111.3(5)
C(7)–Os(3)–C(9)	100.4(5)	C(48)–Os(6)–C(50)	99.6(6)
C(6)–Os(2)–Os(1)	93.2(3)	C(41)–Os(4)–Os(5)	91.6(4)
C(35)–P(2)–Os(2)	112.8(3)	C(57)–P(3)–Os(4)	116.9(3)
C(29)–P(2)–Os(2)	119.7(3)	C(51)–P(3)–Os(4)	119.8(3)
C(28)–P(2)–Os(2)	112.8(3)	C(63)–P(3)–Os(4)	112.2(3)

opposite directions of the axial CO ligands and out of plane positioning of the CCSCCSCC ring atoms (Figure 6). The two molecules are not related by crystallographic symmetry

because of their pronounced conformational flexibility and therefore can be described as deformation isomers of enantiomers. The discussion below is focused on one of the two molecules [Os(4) to Os(6) (molecule 2)] since the main structural features are similar. Cluster **3** consists of a triangular triosmium cluster with 10 terminal carbonyl ligands and one PSSP ligand. The two phosphine moieties occupy equatorial sites on different osmium atoms with the phosphorus atoms coordinated in a *cis,trans* mode to the bridged metal atoms [Os(1)–Os(2) and Os(4)–Os(5) for molecules 1 and 2, respectively]. The interconnecting aliphatic chain, including the two thioether moieties, is oriented in a zigzag form away from the metal plane. The sulfur atoms are not at bonding distance to any osmium atom. The two Os–Os bonds *cis* to Os(5)–P(4) and Os(4)–P(3) [Os(4)–Os(5) 2.9051(6) Å, Os(4)–Os(6) 2.9087(6) Å] are slightly longer than the Os–Os bond *trans* to the Os(5)–P(4) bond [Os(5)–Os(6) 2.8889(6) Å], which is similar to the average Os–Os distance in $[\text{Os}_3(\text{CO})_{12}]$ [Os–Os_{av} 2.877 Å].²⁸ An analogous trend has been observed for the *cis,trans* isomer of $[\text{Os}_3(\text{CO})_{10}(\text{PPh}_3)_2]$.²⁴ In the latter molecule, the two bonds in *cis* position to the phosphines are internally different, while in **3** there is no significant difference between these bonds. It should be noted that also the bridged Os–Os bonds in the compounds $[\text{Os}_3(\text{CO})_{10}(\mu\text{-Ph}_2\text{P}(\text{CH}_2)_n\text{PPh}_2)]$ ($n = 2, 4, 5$)^{24,25} and $[\text{Os}_3(\text{CO})_{10}(\mu\text{-PSP})]$ (PSP = $\{\text{Ph}_2\text{PCH}_2\text{CH}_2\}_2\text{S}$)⁹ are longer than the other two Os–Os bonds.

The osmium–phosphorus distances in **3** [Os(1)–P(1) 2.358(3) Å, Os(2)–P(2) 2.338(3) Å] fall in the range 2.28–2.40 Å, which is typical for $[\text{Os}_3(\text{CO})_{12-x}(\text{L})_x]$ ($x = 1-3$, L = phosphine) species.²⁰ The Os–P bond *cis* to the bridged metal–metal bond is slightly longer than the other phosphorus–osmium bond. This difference in bond length may be explained as the combined effect of steric repulsions between the interconnecting $\{(\text{CH}_2)_2\text{S}(\text{CH}_2)_2\text{S}(\text{CH}_2)_2\}$ moiety and the asymmetric coordination of the phosphine groups. The Os–P distances in the *cis,trans* isomer of $[\text{Os}_3(\text{CO})_{10}(\text{PPh}_3)_2]$ ²⁴ are also slightly different. Both phosphorus atoms are slightly displaced out of the Os₃ planes [P(1) ca. +0.272 Å, P(2) ca. +0.592 Å, P(3) ca. +0.693 Å, and P(4) ca. +0.144 Å].

In Figure 7, the relative orientation of the equatorial ligands of **3** is compared to that in $[\text{Os}_3(\text{CO})_{10}(\text{PPh}_3)_2]$. In **3**, the equatorial substituents at Os(4) are twisted toward Os(5) when compared to the corresponding orientation in $[\text{Os}_3(\text{CO})_{10}(\text{PPh}_3)_2]$. This twist may be caused by steric restrictions of the interconnecting chain in the PSSP ligand. Thus, in **3** the phosphorus atom *trans* to the bridged metal–metal bond assumes an almost linear position relative to the bridged osmium atoms [P(3)–Os(4)–Os(5) = 162.15(7)°]. The distortion is also accompanied by a narrowing of the C(41)–Os(4)–Os(5) angle [C(41)–Os(4)–Os(5) 91.6(4)° compared to 99.65(16)° for *cis,trans*- $[\text{Os}_3(\text{CO})_{10}(\text{PPh}_3)_2]$]. The average *cis* torsion angle derived from the six A(ax)–Os–Os–A(ax) (A = axially coordinated C and S atoms) dihedral intersections is less than the corresponding average *cis* torsion angle for $[\text{Os}_3(\text{CO})_{10}(\mu\text{-PSP})]$ but near the value for $[\text{Os}_3(\text{CO})_{10}(\text{PPh}_3)_2]$ [26.5° vs 32.3° and 24.4°]. The difference in the twisting of the cluster ligand spheres in **3** and $[\text{Os}_3(\text{CO})_{10}(\mu\text{-PSP})]$ may be explained by the fact that in **3** the phosphines are coordinated in a *cis,trans* mode, while in cluster $[\text{Os}_3(\text{CO})_{10}(\mu\text{-PSP})]$ the two phosphine groups coordinate in a *cis* mode. The coordination that results in the least steric interactions between the ligands is when the

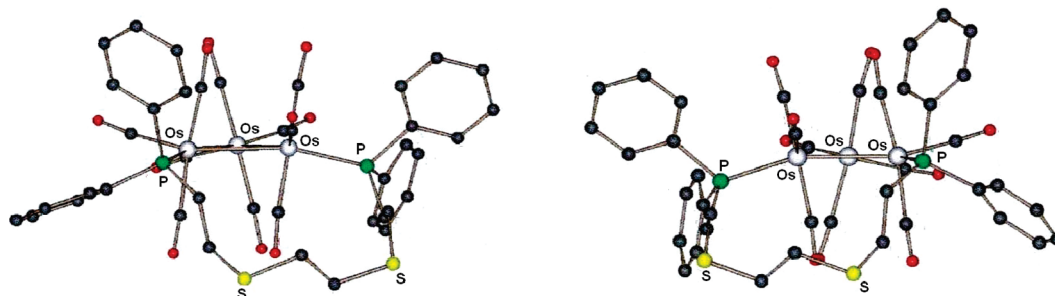


Figure 6. Side view of the two independent molecules in the crystal structure of 1,2-[Os₃(CO)₁₀(PSSP)]₂, **3**, showing the conformation of the 12-membered metallacycle and the tilting of the carbonyl ligands relative to the triangular metal plane.

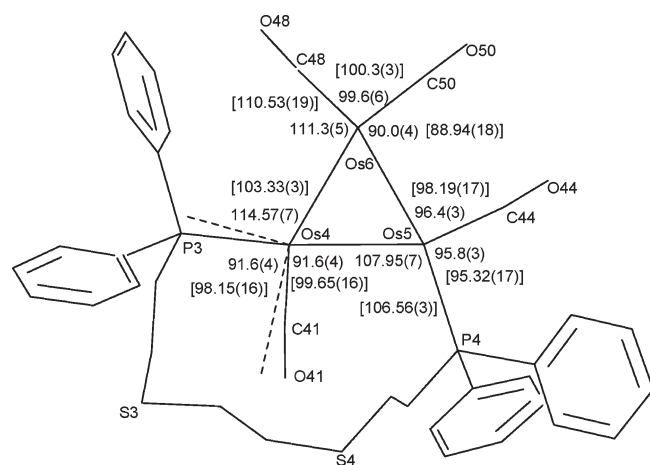


Figure 7. Comparison of the framework structures of [$\{\text{Os}_3(\text{CO})_{10}\}_2(\mu\text{-PSSP})$], **4**, and *cis,trans*-[Os₃(CO)₁₀(PPh₃)₂]. Dotted lines show the principal position of the stereorelated PPh₃ ligand and the geminal equatorial carbonyl group in *cis,trans*-[Os₃(CO)₁₀(PPh₃)₂]. Values within square brackets are corresponding angles in *cis,trans*-[Os₃(CO)₁₀(PPh₃)₂].

phosphines are coordinated in *trans* position (see Figure 4). The *cis,trans* coordination found in **3** is also more sterically favored than the *cis,cis* mode. The carbon–osmium distances for the axial carbonyl ligands (Os–C(av) = 1.94 Å [1.90 Å for molecule 2]) are slightly longer than the carbon–osmium distances for carbonyl ligands in equatorial positions (Os–C(av) = 1.89 Å [1.88 Å for molecule 2]) as commonly found in triosmium clusters.

Ligand Fluxionality in [Os₃(CO)₁₀(μ -PSSP)] (3**).** As mentioned above, the fluxional process in **3** that was detected by ³¹P NMR could be frozen out at low temperature (Figure 3), and the static spectrum shows three resonances at δ –5.5, –9.4, and –10.1. By taking into account their relative intensity, it is straightforward to conclude that the peaks at δ –5.5 and –9.4 are associated with the main isomer, whereas the resonance at δ –10.1 is associated with a minor isomer. The resonances of the main isomer start to broaden at 233 K and coalesce at about 285 K with an activation energy of 51.6 kJ/mol. In order to gain a better understanding of this fluxional process, we undertook a ¹³C{¹H} variable-temperature study of **3**. The low-temperature limiting natural abundance ¹³C{¹H} spectrum of **3** (400 MHz, 213 K, CDCl₃) shows 10 distinct CO resonances at δ 200.5 *h/i* (²J_{P–C} \approx 8 Hz), 195.4 *i/h* (²J_{P–C} \approx 8 Hz), 192.5 *a/b* (²J_{P–C} \approx 9 Hz), 192.0 *b/a* (²J_{P–C} \approx 6 Hz), 185.8 *d/e*, 185.4 *e/d*, 183.5 *j/f*, 178.7 *c/g*, 174.0 *g/c*, and 172.1 *f/j* (see Figure 8). The four low-frequency resonances may be assigned to the equatorial

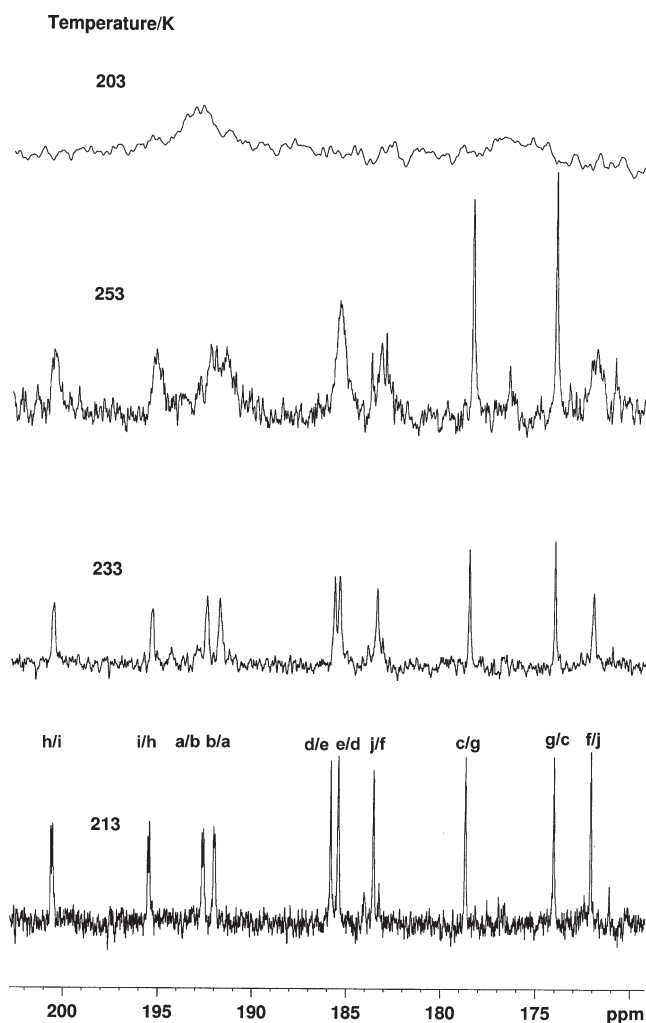
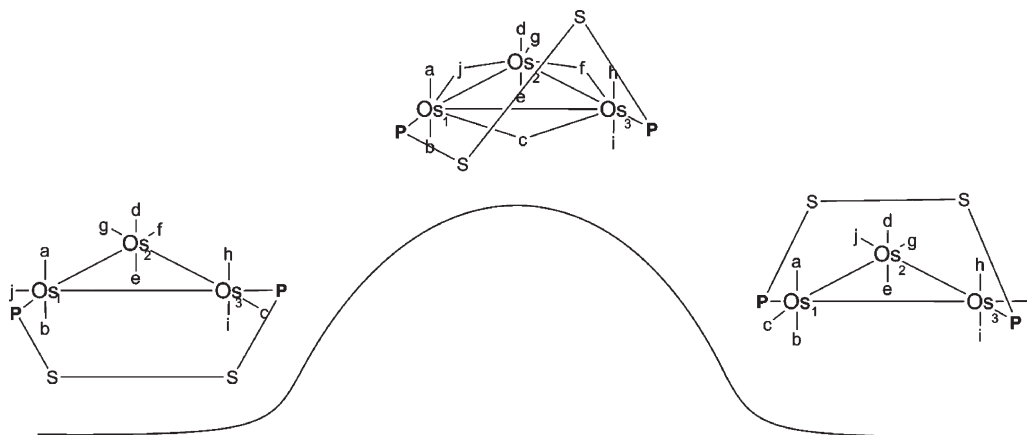


Figure 8. Low-temperature limiting natural abundance ¹³C{¹H} spectrum of 1,2-[Os₃(CO)₁₀(PSSP)]₂, **3** (400 MHz, 213 K, CDCl₃).

carbonyls, and the four signals at highest frequency are unambiguously assigned as the axial carbonyl ligands of the two phosphine-coordinated osmium atoms, on the basis of the large observed ²J_{P–C} couplings. The X-ray structure of **3** (*vide supra*) shows that the aliphatic chain is oriented away from the metal plane in the solid state, and this is the reason for a significant chemical shift difference of the pairs of axial carbonyls bound to the same osmium atoms. The unusual high frequency of the carbonyl resonance at δ 200.5 suggests that there may be some interaction between the ligand and this CO. We tentatively propose the presence of a steric

Scheme 3. Proposed Fluxional Process for **3**

sulfur–CO interaction that affects the energy barrier for the fluxional process.

On increasing the temperature to 253 K, eight of the 10 signals broaden. However, two equatorial carbonyls (δ 178.7 and 174.0) remain sharp. A value of 50.6 ± 2.0 kJ/mol for the carbonyl exchange activation energy has been estimated from line-shape analysis, in reasonable agreement with the activation energy found for phosphorus exchange (see below).

The observed mutual exchange of the phosphorus and the behavior of the VT ^{13}C spectra in the temperature range 213–253 K can be explained as follows (see Scheme 3): a rapid switch forward and backward of the two phosphorus atoms leads to a restricted and concerted motion of the carbonyl ligands in the equatorial plane of the metal triangle, probably through a higher energy intermediate state having bridging CO ligands. This motion is responsible for the mutual exchange of the phosphorus atoms and for the pairwise exchange of equatorial carbonyls *f* and *j*. It is worth noting that carbonyls *c* and *g* appear static on the NMR time scale, since they are moving between chemically equivalent positions. Moreover, the PSSP chain is expected to possess considerable flexibility, and large-amplitude conformational changes in the 12-membered ring/“dimetallacycle” “may remove the asymmetry of the metal plane, causing also pairwise exchange of the axial carbonyls *a/b*, *h/i*, *d/e*. These two concomitant motions fully explain the line broadening of all carbonyl resonances, except *c* and *g*, observed at 253 K. A classical terminal/bridge exchange process in the vertical plane is unlikely to occur since that would induce considerable steric interactions of the R groups (in this case phenyl rings) of the phosphines with the two axial carbonyls on the same side of the osmium plane.

At 303 K, the resonances *c* and *g* are also broad, revealing further dynamic processes. It is interesting to observe that at 303 K the broad peak in the higher frequency region represents the average value of the six axial carbonyls. This rather unexpected result can be rationalized only with a migration of the PSSP ligand in the equatorial plane that involves all three osmium atoms. The small peak at δ -10.1 in the ^{31}P spectra (and the occurrence of several small resonances in the ^{13}C spectra) are related to the presence of the *trans,trans* or the *cis,cis* isomer.

Properties of $[\{\text{Os}_3(\text{CO})_{10}\}_2(\mu\text{-PSSP})]$ (4**).** The IR spectrum of $[\{\text{Os}_3(\text{CO})_{10}\}_2(\mu\text{-PSSP})]$, **4**, is similar to that observed for P,S-bridged triosmium clusters,^{8,9} indicating similar symmetry of the carbonyl ligands. The room-tem-

perature $^{31}\text{P}\{^1\text{H}\}$ NMR shows a sharp resonance at δ -0.06 , indicating a single phosphorus environment and that no fluxional process involving phosphorus is present at this temperature. The $^{31}\text{P}\{^1\text{H}\}$ NMR chemical shift δ -0.057 is very similar to that of the compound $1,2\text{-}[\text{Os}_3(\text{CO})_{10}(\mu\text{-Ph}_2\text{PCH}_2\text{CH}_2\text{SMe})]$ ⁸ (δ $= -0.597$), indicating a similar magnetic environment for the P atoms in **4** to that in $1,2\text{-}[\text{Os}_3(\text{CO})_{10}(\mu\text{-Ph}_2\text{PCH}_2\text{CH}_2\text{SMe})]$. Furthermore, the presence of only one resonance in the spectrum indicates that the ligand is symmetrically coordinated. In the ^1H NMR spectrum, three multiplets are present at δ 2.3, 2.5, and 2.8 and a broad envelope in the region between δ 7.3 and 7.4. These signals were assigned to the aliphatic (δ 2.3–2.8) and aromatic (δ 7.3–7.4) protons of PSSP, with relative ratios of 20:12, indicating that the ligand is intact in the cluster. The compound is stable at room temperature and on heating in refluxing dichloromethane for one hour. Considering the similarity of the spectroscopic data of **4** and $1,2\text{-}[\text{Os}_3(\text{CO})_{10}(\mu\text{-Ph}_2\text{PCH}_2\text{CH}_2\text{SMe})]$,⁸ compound **4** is expected to consist of two P,S-bridged cluster units as shown in Figure 9.

We have previously observed that P,S-ligands initially coordinate in a bridging coordination mode along one edge of an Os_3 cluster unit but rearrange under mild conditions to a chelating coordination mode, with the ligands remaining intact throughout the rearrangement process.⁸ A similar rearrangement from a 1,2-bridging to a 1,1-chelating coordination mode has been observed for the triosmium carbonyl derivatives of the unsaturated symmetrical diphosphine ligands 4,5-bis(diphenylphosphino)-4-cyclopentene-1,3-dione (bpcd), (*Z*)- $\text{Ph}_2\text{PCH}=\text{CHPPh}_2$, and 2,3-bis(diphenylphosphino)-*N-p*-tolylmaleimide (bmi).²⁷ Both phosphine donor atoms occupy equatorial coordination sites in the thermodynamic products of these reactions. Furthermore, similar rearrangements have been detected for $[\text{H}_4\text{Ru}_4(\text{CO})_{10}(\text{P}-\text{P})]$ (P–P = diphosphine) clusters.²⁸ Upon storage in dichloromethane solution for several days, a singlet at δ 40.2 ppm could be observed in the ^{31}P NMR spectrum of **4**, but the conversion never went to completion in our experiments. The singlet is close in chemical shift to that at δ 41.5 found for the cluster $1,1\text{-}[\text{Os}_3(\text{CO})_{10}(\mu\text{-Ph}_2\text{PCH}_2\text{CH}_2\text{SMe})]$, and we suggest that the new resonance is better explained as an effect of the presence of one or both of the isomers depicted in Figure 10. Spectroscopic data for the cluster $1,1\text{-}[\{\text{Os}_3(^{13}\text{CO})_{11}\}(\mu\text{-PSP})\text{-}\{\text{Os}_3(\text{CO})_{10}\}]$ ⁹ indicate that the P,S-chelated $\{\text{Os}_3(\text{CO})_{10}\}$ unit is sterically restricted in its movement relative to the phosphorus-coordinated $\{\text{Os}_3(^{13}\text{CO})_{11}\}$ unit. Considering that

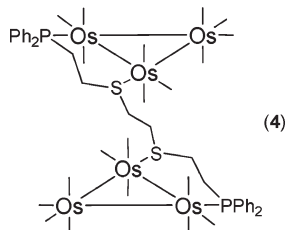


Figure 9. Proposed structure for $[\{\text{Os}_3(\text{CO})_{10}\}_2(\text{PSSP})]$, **4**.

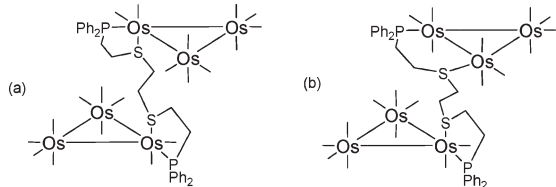


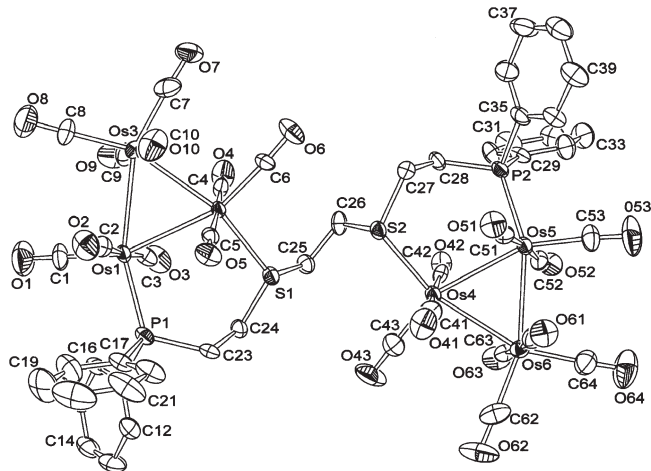
Figure 10. Proposed isomers of $[\{\text{Os}_3(\text{CO})_{10}\}_2(\text{PSSP})]$, **4**, in which one or both of the phosphine thioether pairs are chelating one of the osmium atoms in each of the triosmium triangles.

cluster **4** consists of two bridged $\{\text{Os}_3(\text{CO})_{10}\}$ units, it is thus likely that the $\{\text{Os}_3(\text{CO})_{10}\}$ units of this compound are also restricted in their movements. In contrast to the cluster $1,2\text{-}[\text{Os}_3(\text{CO})_{10}(\mu\text{-Ph}_2\text{PCH}_2\text{CH}_2\text{SMe})]$, **4** is relatively stable. This may be explained by steric hindrance increasing the barrier for the 1,2-bridging to 1,1-chelating rearrangement in **4**. In spite of repeated attempts, we were unable to get pure samples of the chelated cluster isomer(s), and therefore no complete characterization of this compound(s) could be achieved.

Crystal and Molecular Structure of $[\{\text{Os}_3(\text{CO})_{10}\}_2(\mu\text{-PSSP})]$ (4**).** The molecular structure of **4** is shown in Figure 11, and relevant bond lengths and angles are reported in Table 3. In cluster **4** the PSSP ligand coordinates to two different triosmium units. In each of the triosmium units, one phosphorus and one sulfur atom of the PSSP ligand are coordinated to different metals in a 1,2-bridging mode with the phosphine and the thioether groups residing *cis* to each other, thus generating two equivalent six-membered rings. All donor atoms are coordinated in equatorial sites, but lie slightly out of the two triangular metal planes [distance from the $\text{Os}(1)\text{--Os}(3)$ plane: $\text{S}(1) -0.12 \text{ \AA}$, $\text{P}(1) +0.65 \text{ \AA}$; distances from the $\text{Os}(4)\text{--Os}(6)$ triangle: $\text{S}(2) -0.65 \text{ \AA}$, $\text{P}(2) +0.49 \text{ \AA}$].

The $\text{Os}\text{--P}$ distances [$\text{Os}(1)\text{--P}(1)$ $2.339(3) \text{ \AA}$, $\text{Os}(5)\text{--P}(2)$ $2.3388(3) \text{ \AA}$] are slightly longer than the $\text{Os}\text{--P}$ distance in $1,2\text{-}[\text{Os}_3(\text{CO})_{10}(\mu\text{-Ph}_2\text{PCH}_2\text{CH}_2\text{SMe})]$ [$\text{Os}\text{--P}$ $2.322(3) \text{ \AA}$] but still within the range that is typical for compounds of formula $[\text{Os}_3(\text{CO})_{12-x}(\text{L})_x]$ ($x = 1, 2, 3$; $\text{L} = \text{phosphine}$).²⁰ The $\text{Os}\text{--S}$ [$\text{Os}(2)\text{--S}(1)$ $2.371(2) \text{ \AA}$, $\text{Os}(4)\text{--S}(2)$ $2.390(2) \text{ \AA}$] separations are slightly different. The shorter $\text{Os}(2)\text{--S}(1)$ interaction is similar to the $\text{Os}\text{--S}$ separation in the cluster $1,2\text{-}[\text{Os}_3(\text{CO})_{10}(\mu\text{-Ph}_2\text{PCH}_2\text{CH}_2\text{SMe})]$ [$\text{Os}\text{--S} = 2.376(3) \text{ \AA}$].⁸ The difference in $\text{Os}\text{--S}$ bond lengths between $\text{Os}(4)\text{--S}(2)$ and $\text{Os}(2)\text{--S}(1)$ may be the result of the fact that the sulfur atom $\text{S}(2)$ is much more displaced out of the metal plane. Spectroscopic data for compound **4** indicate that the cluster is symmetric (*vide supra*), and therefore it is likely that the difference in bond lengths is a solid-state phenomenon that may be related to crystal packing effects.

The average $\text{Os}\text{--Os}$ distances in the M_3 triangles [$\text{Os}\text{--Os}(\text{av}) = 2.861 \text{ \AA}$ for $\text{Os}(1)\text{Os}(2)\text{Os}(3)$ and 2.860 \AA for $\text{Os}(4)\text{--}$



source of this effect, as the two out-of-phase combinations of lone pairs on the sulfur and the phosphorus require an antibonding combination of Os orbitals, resulting in a destabilization of the bridged Os–Os bond. The Os–Os bonds *trans* to the sulfur in each of the M_3 units of **4** are the shortest ones [Os(2)–Os(3) 2.8317(6) Å and Os(4)–Os(6) 2.8422(6) Å], while the metal–metal bonds *trans* to the phosphorus atoms are slightly longer. A contraction of the metal–metal bond *trans* to the sulfur has been observed in related clusters.³⁰

The structure of cluster **4** is closer to D_3 symmetry than that of the related compound 1,2-[Os₃(CO)₁₀(μ-Ph₂PCH₂CH₂SMe)].⁸ The average *cis* torsion angle derived from the six A(ax)–Os–Os–A(ax) (A = axially coordinated C atoms) dihedral intersections is considerably larger than for 1,2-[Os₃(CO)₁₀(μ-Ph₂PCH₂CH₂SMe)] but slightly narrower than for the bridged isomer [Os₃(CO)₁₀(μ-PSP)]⁹ [26.7° for Os(1)–Os(3), 27.5° for Os(4)–Os(6) vs 11.7° for 1,2-[Os₃(CO)₁₀(μ-Ph₂PCH₂CH₂SMe)] and 32.3° for [Os₃(CO)₁₀(μ-PSP)]]. Both **4** and 1,2-[Os₃(CO)₁₀(μ-Ph₂PCH₂CH₂SMe)] have very similar coordination motifs. The reason for the twist of the cluster ligand spheres in both M_3 units of **4** may be ascribed to the combined effect of conformational requirements due to mutual interactions between the sterically demanding {Os₃(CO)₁₀PPh₂(CH₂)₂SCH₂} moieties of **4** and packing effects in the solid state. Conformational isomerism in the solid state has been observed for the compound [Os₃(CO)₁₁(PR₃)] (R = *p*-C₆H₄F), which exists in a red and yellow form in the solid state.³¹ The yellow isomer has a typical D_{3h} -like structure as for Os₃(CO)₁₁(L) (L = phosphine or phosphite) species, whereas in the red form the neighboring carbonyls on adjacent Os atoms are in a staggered configuration, resulting in a D_3 -like structure. The close similarities between **4** and the cluster 1,2-[Os₃(CO)₁₀(μ-Ph₂PCH₂CH₂SMe)] indicate that only a subtle change of structure may change the ligand polyhedron from D_{3h} to D_3 and *vice versa*. The interchange between D_{3h} and D_3 may also be controlled by thermodynamics of the crystallization process.

Conclusions. We have found that the mixed ligand PSSP easily coordinates to activated triosmium clusters. We have prepared and structurally characterized four new clusters; in three of these (clusters **1**–**3**), the PSSP ligand coordinates only via its phosphine donor atoms. The molecular structure of **3** shows that the two phosphine moieties occupy equatorial sites on different osmium atoms with the phosphorus atoms coordinated in a *cis,trans* mode to the bridged metal atoms. To our knowledge, this is the first example of bridging coordination of a bi- or polydentate ligand to a [M₃(CO)₁₂] cluster (M = Ru, Os) where the ligand is bridging in a *cis,trans* mode. The cluster [Os₃(CO)₁₀(μ-PSSP)], **3**, is fluxional on the NMR time scale; this fluxionality involves movement of the phosphine moieties in the equatorial plane, coupled with carbonyl exchange in the equatorial plane and a “flip” of the ligand backbone.

The solid-state structure of **4** reveals that the compound consists of two P,S-coordinated {Os₃(CO)₁₀} subunits linked by a PSSP ligand. Cluster **4** is relatively stable, in contrast to what has been observed for the analogous compounds 1,2-[Os₃(CO)₁₁](μ-PSP){Os₃(CO)₁₀}⁹ and 1,2-[Os₃(CO)₁₀(μ-Ph₂

PCH₂CH₂SMe)],⁸ but prolonged standing in solution leads to the formation of a new cluster, which is suggested to be a stable isomer of **4** in which the PSSP ligand is chelating an osmium atom in each of the triosmium triangles.

Experimental Section

General Procedures. The clusters [Os₃(CO)₁₂],³² [Os₃(CO)₁₁(NCMe)],³³ and [Os₃(CO)₁₀(NCMe)₂]³⁴ were synthesized by published methods. The ligand PSSP was synthesized, as reported previously.³⁵ All reactions were carried out under an atmosphere of dry nitrogen using standard Schlenk and vacuum-line techniques. Solvents were dried by standard methods prior to use. Infrared spectra were recorded as solutions in 0.5 mm NaCl cells on Nicolet 20SXC and Avatar 360 FT-IR spectrometers with carbon dioxide as calibrant. Fast atom bombardment (FAB) mass spectra were obtained on a JEOL SX-102 spectrometer using 3-nitrobenzyl alcohol as matrix and CsI as calibrant. ¹H NMR spectra (299.87 MHz) were acquired on a Varian Unity 300 WB spectrometer; ¹H (500.13 MHz), ³¹P{¹H} (200.25 MHz), and ¹³C{¹H} NMR (125 MHz) spectra were acquired on a Bruker DRX 500 spectrometer. Routine separations of products were performed by thin-layer chromatography using commercially prepared glass plates, precoated with 0.25 mm Merck silica gel 60. Column chromatography was carried out using silica gel (Merck silica gel 60, 0.040–0.063 mm, 230–400 mesh, ASTM) columns, initially packed in CH₂Cl₂.

Synthesis of [{Os₃(CO)₁₁]₂(μ-PSSP)] (1). In a typical reaction, 194 mg (0.107 mmol) of [Os₃(CO)₁₁(NCMe)] and 56 mg (0.057 mmol) of PSSP were dissolved in 20 mL of CH₂Cl₂ and stirred at room temperature until no ν_{C–O} resonances due to the starting material could be detected (2h). The solvent was then removed under reduced pressure, and residual solid was separated by TLC using thf/hexane (3:7 v/v) as eluent, yielding two bands, in order of decreasing *R_f*: [{Os₃(CO)₁₁]₂(μ-PSSP)] (**1**), yellow, 108 mg (0.0623 mmol, 43%), and traces of **2**. Cluster **1**: IR ν(CO), cm⁻¹ (cyclohexane): 2108m, 2069m, 2056s, 2036s, 2021vs, 2004m, 1992m, 1980m. ¹H NMR (CDCl₃, 303 K): δ 2.27m, 2.49m, 2.82m. ¹³P{¹H} NMR (CDCl₃, 303 K) (H₃PO₄: δ = 0; positive shift at higher frequency): δ -10.92. Anal. Calcd (found) for **1**: H 1.42 (1.54), C 27.44 (29.09), P 2.72 (2.67). FAB+ MS (*m/z*): 2276 (M⁺).

Synthesis of [Os₃(CO)₁₁(PSSP)] (2). In a typical reaction, 100 mg (0.100 mmol) of [Os₃(CO)₁₁(NCMe)] was dissolved in 20 mL of dichloromethane. A 113 mg (0.218 mmol) amount of PSSP was added to the solution. The solution was stirred at room temperature for 1.5 h under nitrogen. The solvent was removed under vacuum, and the crude product was separated by thin-layer chromatography using a 7:3 hexane/CH₂Cl₂ mixture as eluent. Two bands were recovered, in order of decreasing *R_f*: [{Os₃(CO)₁₁]₂(μ-PSSP)] (**1**) (minor trace); [Os₃(CO)₁₁(PSSP)] (**2**), yellow, 20 mg (0.009 mmol, 9%). Cluster **2**: IR (cyclohexane), ν(CO)/cm⁻¹: 2108m, 2055s, 2018vs, 1988m. ¹H NMR (CDCl₃, 303 K): 2.30 (m, 4H), 2.53 (m, 4H), 2.84 (m, 4H), 7.25–7.46 (m, 20H). ¹³C{¹H} NMR (125 MHz, 213 K, CDCl₃): 193.1 (d, ²J_{P–C} = 7.9 Hz, 2C), 185.4 (s, 2C), 183.9 (s, 2C), 176.8 (s, 1C), 176.7 (s, 1C), 172.8 (s, 1C), 172.4 (s, 1C), 170.2 (s, 1C). ¹³P{¹H} NMR (CDCl₃, 303 K) (H₃PO₄: δ = 0): δ -17.3 (s, 1P), -10.2 (s, 1P). FAB+ MS (*m/z*): 1426 (M⁺) Anal. Calcd (found) for **2**: H 2.31 (2.26), C 35.24 (35.40), P 4.43 (4.84).

Synthesis of [Os₃(CO)₁₀(μ-PSSP)] (3). A 100 mg (0.107 mmol) amount of [Os₃(CO)₁₀(NCMe)₂] and 139 mg (0.268 mmol) of

(30) (a) Adams, R. D.; Horvath, I. T.; Segmüller, B. E.; Yang, L. Y. *Organometallics* **1983**, *2*, 144. (b) Kiriakidou-Kazemifar, N. K.; Kretzschmar, E.; Carlsson, H.; Monari, M.; Selva, S.; Nordlander, E. *J. Organomet. Chem.* **2001**, *623*, 191.

(31) Hansen, V. M.; Ma, A. K.; Biradha, K.; Pomeroy, R. K.; Zaworotko, M. J. *Organometallics* **1998**, *17*, 5267.

(32) Johnson, B. F. G.; Lewis, J. *Inorg. Synth.* **1972**, *13*, 93.

(33) Johnson, B. F. G.; Lewis, J.; Pippard, D. A. *J. Chem. Soc., Dalton Trans.* **1978**, *C4*, 407.

(34) Nicholls, J. N.; Vargas, M. D. *Inorg. Synth.* **1989**, *26*, 289.

(35) (a) Degischer, G.; Schwarzenbach, G. *Helv. Chim. Acta* **1966**, *49*, 1927. (b) Hsiao, Y.-M.; Chojnacki, S. S.; Hinton, P.; Reibenspies, J. H.; Darensbourg, M. Y. *Organometallics* **1993**, *12*, 870.

Table 4. Crystal Data and Experimental Details for $[\{\text{Os}_3(\text{CO})_{11}\}_2(\mu\text{-PSSP})]$ (**1**), $[\text{Os}_3(\text{CO})_{10}(\mu\text{-PSSP})]$ (**3**), and $[\{\text{Os}_3(\text{CO})_{10}\}_2(\mu\text{-PSSP})] \cdot 2\text{CHCl}_3$ (**4**) ($2 \cdot 2\text{CHCl}_3$)

	1	3	4
formula	$\text{C}_{52}\text{H}_{32}\text{O}_{22}\text{Os}_6\text{P}_2\text{S}_2$	$\text{C}_{40}\text{H}_{32}\text{O}_{10}\text{Os}_3\text{P}_2\text{S}_2$	$\text{C}_{50}\text{H}_{32}\text{O}_{20}\text{Os}_6\text{P}_2\text{S}_2 \cdot 2\text{CHCl}_3$
<i>M</i>	2276.04	1369.35	2458.75
temp, K	100(2)	293(2)	293(2)
wavelength, Å	0.71073	0.71073	0.71073
cryst symmetry	triclinic	monoclinic	triclinic
space group	$P\bar{1}$	$P2_1$	$P\bar{1}$
<i>a</i> , Å	13.5001(15)	11.8958(5)	13.9222(6)
<i>b</i> , Å	16.0441(16)	18.4288(7)	15.5954(7)
<i>c</i> , Å	16.7391(16)	19.8714(8)	17.5669(8)
α , deg	112.960(3)	90	109.624(1)
β , deg	103.163(3)	100.883(1)	99.645(2)
γ , deg	105.503(3)	90	104.675(2)
cell volume, Å ³	2983.1 (5)	4278.0(3)	3339.2(3)
<i>Z</i>	2	4	2
<i>D</i> _c , Mg m ⁻³	2.534	2.126	2, 2.445
$\mu(\text{Mo K}\alpha)$, mm ⁻¹	12.93	9.115	11.789
<i>F</i> (000)	2076	2568	2252
cryst size, mm	0.30 × 0.10 × 0.08	0.30 × 0.25 × 0.20	0.28 × 0.25 × 0.23
θ limits, deg	1.8–25.0	1.04–30.03	2.56–29.99
reflns collected	16 593	58 470	45 638
unique obsd reflns	10 441	24 914	19 363
$[F_o > 4\sigma(F_o)]$			
absolute struct param		−0.035(6)	
goodness of fit on <i>F</i> ²	1.10	0.820	0.901
<i>R</i> ₁ (<i>F</i>) ^a	0.0960, 0.2543	0.0422, 0.0670	0.0471, 0.1002
<i>wR</i> ₂ (<i>F</i> ²) ^b			
largest diff peak and hole, e Å ⁻³	6.52 and −7.33	1.479 and −1.286	3.336 and −1.762

$$^a R_1 = \sum |F_o| - |F_c| / \sum |F_o|, \quad ^b wR_2 = [\sum w(F_o^2 - F_c^2)^2 / \sum w(F_o^2)^2]^{1/2} \text{ where } w = 1/[\sigma^2(F_o^2) + (aP)^2 + bP] \text{ where } P = (F_o^2 + F_c^2)/3.$$

PSSP were dissolved in ca. 100 mL of CH_2Cl_2 . The solution was stirred under nitrogen for 1.5 h. The solvent was then removed under reduced pressure, and the crude product was separated by thin-layer chromatography using a 3:7 thf/*n*-hexane mixture as eluent. Two bands were recovered, in order of decreasing *R*_f: $[\text{Os}_3(\text{CO})_{10}(\mu\text{-PSSP})]$ (**3**), red 51.9 mg (0.02 mmol, 35%), and a yellow, uncharacterized compound. Cluster **3**: IR (CH_2Cl_2), $\nu(\text{CO})/\text{cm}^{-1}$: 2086m, 2021sh, 2000vs, 1973w, 1950w-m. ¹H NMR (CDCl_3 , 303 K): 2.18m, 2.6–3.2m, 3.74m, 7.45–7.71m. ¹³C{¹H} NMR (CDCl_3 , 213 K): 200.5 (d, ²*J*_{P-C} ≈ 8 Hz, 1C), 195.4 (d, ²*J*_{P-C} ≈ 8 Hz, 1C), 192.5 (²*J*_{P-C} ≈ 9 Hz, 1C), 192.0 (²*J*_{P-C} ≈ 6 Hz, 1C), 185.8 (s, 1C), 185.4 (s, 1C), 183.5 (s, 1C), 178.7 (s, 1C), 174.0 (s, 1C), and 172.1 (s, 1C). ³¹P{¹H} NMR (500 MHz, CDCl_3 , 213 K) (H_3PO_4 : $\delta = 0$): −5.5 (s), −9.4 (s), −10.1 (s). Anal. Calcd (found) for **3**: H 2.36 (2.59), C 35.09 (37.04). FAB+ MS (*m/z*): 1369, calculated from the parent molecular ion 1370.

Synthesis of $[\{\text{Os}_3(\text{CO})_{10}\}_2(\mu\text{-PSSP})]$ (4**).** In a typical reaction a solution of 3.7 equiv of Me_3NO (6.4 mg, 0.058 mmol) dissolved in dry CH_2Cl_2 was added dropwise to a stirred dichloromethane solution (50 mL) of $[\{\text{Os}_3(\text{CO})_{11}\}_2(\mu\text{-PSSP})]$ (50 mg, 0.023 mmol) at room temperature. The reaction was monitored by IR spectroscopy. The solvent was removed under reduced pressure, and the residual solid was separated by preparative TLC (0.5 mm, Merck 1045) eluting with a thf/hexane mixture (3:7 by volume). The orange, major product **4** (60 mg, 0.03 mmol, 60%) was recovered and identified as $[\{\text{Os}_3(\text{CO})_{10}\}_2(\mu\text{-PSSP})]$. A minor, orange-red product **5** was also recovered and identified as $[\{\text{Os}_3(\text{CO})_{10}\}(\mu\text{-PSSP})]$. Cluster **4**: IR (CH_2Cl_2), $\nu(\text{CO})/\text{cm}^{-1}$: 2090vs, 2029w, 2007vs, 1975m, 1954m. ¹H NMR (CDCl_3 , 293 K): 2.23–2.28 (m, 4H), 2.47–2.53 (m, 4H), 2.7–2.9 (m, 4H), 7.29–7.44 (m, 20H). ³¹P{¹H} NMR (CDCl_3 , 293 K): −0.057 s. FAB+ MS (*m/z*): 1097 (M^+).

Crystallography. Yellow crystals of $[\{\text{Os}_3(\text{CO})_{11}\}_2(\mu\text{-PSSP})]$, **1**, were grown by slow evaporation from a CHCl_3 solution. Red crystals of $[\text{Os}_3(\text{CO})_{10}(\mu\text{-PSSP})]$, **3**, were obtained by slow evaporation from a dichloromethane/*n*-hexane solution. Yellow crystals of $[\{\text{Os}_3(\text{CO})_{10}\}_2(\mu\text{-PSSP})]$, **4**, were grown from a

CHCl_3 solution. Crystal data and experimental details of the data collections and structure refinements for **1**, **3**, and **4** are summarized in Table 4.

X-ray Data Collection and Structure Determination of **1.** Suitable crystals were mounted in inert oil droplets, which solidified at the data collection temperature of 100(2) K on a Nonius Kappa CCD diffractometer. The crystals were indexed and the data collection strategy was determined by the Nonius Collect program.³⁶ Data were integrated, merged, and corrected for Lorentz and polarization effects and for the effects of absorption using the programs DENZO-SMN and Scalepack.³⁷ The structure was solved by direct methods, and all non-hydrogen atoms of the clusters were refined anisotropically (SHELXL-97),³⁸ while hydrogen atoms were included in calculated positions and allowed to ride on the atoms to which they were attached, with thermal parameters tied to those of the parent atom. Details of the crystal data and of the data collection for **1** are reported in Table 4.

X-ray Data Collection and Structure Determination of **3 and **4**.** Crystal data and other experimental details for **3** and **4** are reported in Table 4. The X-ray intensity data for **3** and **4** were measured on a Bruker AXS SMART 2000 diffractometer, equipped with a CCD detector, using Mo K α radiation ($\lambda = 0.71073$ Å) at room temperature. Cell dimensions and the orientation matrix were initially determined from least-squares refinement on reflections measured in three sets of 20 exposures collected in three different ω regions and eventually refined against 5905 reflections. A full sphere of reciprocal space was scanned by 0.3° ω steps with the detector kept at 5.0 cm from the sample. Intensity decay was monitored by re-collecting the initial 50 frames at the end of the data collection and analyzing the duplicate reflections. The collected frames were processed

(36) "Collect" data collection software; B.V. Nonius: Delft, 1998.

(37) Otwinowski, Z.; Minor, W. *Methods in Enzymology*; Carter, C. W.; Sweet, R. M., Eds.; Academic Press: New York, 1996; p 276.

(38) Sheldrick, G. M. *SHELXL-97*; University of Göttingen, 1997.

for integration by using the program SAINT, and an empirical absorption correction was applied using SADABS³⁹ on the basis of the Laue symmetry of the reciprocal space. The structures were solved by direct methods (SIR 97)⁴⁰ and subsequent Fourier syntheses and refined by full-matrix least-squares on F^2 (SHELXTL)⁴¹ using anisotropic thermal parameters for all non-hydrogen atoms. The phenyl and methylene hydrogen atoms were added in calculated positions and refined using isotropic thermal parameter 1.5 and 1.2 times U_{eq} of the carrier carbons. The final refinement on F^2 proceeded by full-matrix least-squares calculations (SHELXL 97) using anisotropic thermal parameters for all the non-hydrogen atoms. For cluster **3** the absolute structure was determined [Flack parameter = $-0.035(6)$]. In cluster **4**, two CHCl_3 molecules are present in

(39) Sheldrick, G. M. *SADABS, program for empirical absorption correction*; University of Göttingen: Germany, 1996.

(40) Altomare, A.; Burla, M. C.; Camalli, M.; Cascarano, G. L.; Giacovazzo, C.; Guagliardi, A.; Moliterni, A. G. G.; Polidori, G.; Spagna, R. SIR97: a new tool for crystal structure determination and refinement. *J. Appl. Crystallogr.* **1999**, *32*, 115.

(41) Sheldrick, G. M. *SHELXTLplus Version 5.1 (Windows NT version)-Structure Determination Package*; Bruker Analytical X-ray Instruments Inc.: Madison, WI, 1998.

the asymmetric unit. Interestingly one of the two Os_3 units [$\text{Os}(1)\text{Os}(2)\text{Os}(3)$] in **4** showed some disorder between $\text{Os}(1)\text{Os}(2)\text{Os}(3)$ and $\text{Os}(1A)\text{Os}(2A)\text{Os}(3A)$, giving rise to a “star of David” arrangement, and the occupancy factors were refined to 0.95 for the major component [$\text{Os}(1)\text{Os}(2)\text{Os}(3)$] and to 0.05 for the minor one [$\text{Os}(1A)\text{Os}(2A)\text{Os}(3A)$].

Acknowledgment. This research was supported by grants from the Swedish Research Council (VR) and the European Union (TMR network Metal Clusters in Catalysis and Organic Synthesis, MECATSYN). B.U. was supported by the Socrates exchange program. M.M. thanks the University of Bologna and MIUR (PRIN2006) for financial support. We would like to thank Dr. Karl-Erik Bergquist for the use of a Bruker DRX500 NMR spectrometer, Prof. Carlaxel Andersson for a generous gift of the PSSP ligand, and Prof. A. J. Deeming for helpful discussions.

Supporting Information Available: Supplementary crystallographic data for compounds **1**, **3**, and **4** (CCDC 717582, 717583, and 717584). This material is available free of charge via the Internet at <http://pubs.acs.org>.